

NAS2-12597

AMES GRANT

IN-02-CR

114232

P.42

**NASA CONTRACTOR
REPORT**

**INTEGRATION OF A SUPERSONIC UNSTEADY
AERODYNAMIC CODE INTO THE NASA
FASTEX SYSTEM**

by Kari Appa and Michael J. C. Smith

Prepared by

**NORTHROP CORPORATION
Aircraft Division
Hawthorne, CA 90250-3277**

for Nasa Ames Research Center

NATIONAL AERONAUTICS AND SPACE ADMINISTRATION - WASHINGTON, D.C. - DECEMBER 1987

**{NASA-CR-182329} INTEGRATION OF A
SUPERSONIC UNSTEADY AERODYNAMIC CODE INTO
THE NASA FASTEX SYSTEM Final Report
(Northrop Corp.) 42 p**

N88-14068

CSCL 01A

**Unclas
G3/02 0114232**

NASA Contractor Report

**INTEGRATION OF A SUPERSONIC UNSTEADY
AERODYNAMIC CODE INTO THE NASA FASTEX SYSTEM**

Kari Appa and Michael J. C. Smith

**Northrop Corporation, Aircraft Division
Hawthorne, California**

**Prepared for
AMES/Dryden Flight Research Center
Under Contract NAS2-12597**

**NASA
National Aeronautics and Space Administration
Scientific and Technical Information Branch
December 1987**

FOREWORD

Integration of a new supersonic unsteady aerodynamic module into the NASA/Ames FASTEX code was performed by Northrop Aircraft Corporation under the NASA Contract NAS2-12597. Dr. K. K. Gupta of NASA/Ames, Dryden Flight Research Center monitored the project. The authors acknowledge the permission of the Air Force (AFWAL/FIBRA) to use the MicroVax II computer system, provided to Northrop as part of the "Automated Strength - Aeroelastic Design of Aerospace Structures" program (F33615-83-C-3232), in the performance of this NASA effort. The authors wish to thank M. J. Brenner of NASA/Ames, Dryden Flight Center for coordinating with the authors during the numerical evaluation, and Dr. W. P. Rodden, Consultant, and J. H. Wykes of the Northrop Aircraft Division for their constructive technical discussions with the authors.

TABLE OF CONTENTS

	<u>Page</u>
LIST OF FIGURES.....	vi
LIST OF TABLES.....	vii
SUMMARY.....	ix
1. INTRODUCTION.....	1
2. MATHEMATICAL MODEL.....	3
3. UPDATING OF THE FASTEX CODE.....	6
4. INPUT DATA MODIFICATIONS.....	11
5. VERIFICATION OF THE SUPERSONIC CODE IN FASTEX.....	12
5.1 The Cornell Flutter Model.....	12
5.2 Stability Derivatives of the X-29 Aircraft.....	13
5.3 Stability Derivatives of an Oblique Wing Research Aircraft.....	15
6. CONCLUSIONS AND RECOMMENDATIONS.....	17
REFERENCES.....	34

PRECEDING PAGE BLANK NOT FILMED

FIGURES

<u>Figure</u>		<u>Page</u>
1	Schematic Diagram of Enhanced FASTEX Code.....	22
2	FASTEX Input Data Format Using Body Panels in Supersonic Flow.....	23
3	Planform of the Cornell Flutter Model.....	27
4	Chordwise Pressure Distribution on the Cornell Wing, $M = 1.135$, $y/b = 0.75$	28
5	Chordwise Pressure Distribution on the Cornell Wing, $M = 1.2$, $y/b = 0.75$	29
6	Flutter Speed and Frequency Versus Number of Boxes Used in the CPM Code for the Cornell Wing.....	30
7	X-29 Modeling for Unsteady Airloads Predictions.....	31
8	Computational Model of an Oblique Wing Research Aircraft.....	32

TABLES

<u>Table</u>		<u>Page</u>
1	Cornell Wing Flutter Analysis and Test Correlation....	18
2	X-29 Longitudinal Stability Derivatives (Rigid A/C)....	19
3	X-29 Lateral Stability Derivatives (Rigid A/C).....	20
4	Stability Derivatives of an Oblique Wing Research Aircraft (Rigid A/C).....	21

SUMMARY

A supersonic unsteady aerodynamic loads prediction method based on the constant pressure method has been integrated into the NASA FASTEX system. The updated FASTEX code can be employed for aeroelastic analyses in subsonic and supersonic flow regimes. A brief description of the supersonic constant pressure panel method, as applied to lifting surfaces and body configurations, is followed by a documentation of updates required to incorporate this method in the FASTEX code. Test cases showing correlations of predicted pressure distributions, flutter solutions and stability derivatives with available data are reported.

1. INTRODUCTION

This report documents the integration of a supersonic unsteady aerodynamic method into the NASA/Ames version of the FASTEX code (Reference 1) operational at Dryden Flight Research Center. The FASTEX code is a modified version of a flutter and strength optimization computer code known as FASTOP (Reference 2). The FASTEX code retains only those features necessary for computing unsteady aerodynamic forces and flutter solutions.

The computation of subsonic unsteady aerodynamic forces in FASTEX utilizes the Doublet Lattice Method (DLM) of Reference 3, whereas in supersonic flow, the Mach box method of Reference 4 was originally employed. The FASTEX version of the Mach box code did not account for interfering effects of multiple lifting surfaces. Therefore, the unsteady airloads on the lifting surfaces which are downstream of a leading lifting surface were computed incorrectly. To predict reliable stability and aeroelastic characteristics of complex aircraft configurations such as the forward swept wing and oblique wing research aircraft, it was deemed necessary to replace the Mach box method by the constant pressure panel method of Reference 5.

The constant pressure panel method employs quadrilateral elements, with a uniform distribution of pressure singularities, whose strengths are determined by the condition of no flow through the surfaces. The computational procedure is similar to that employed in the DLM code; hence the CPM algorithm can utilize the geometry processing of the DLM code, and a unified code becomes available for subsonic and supersonic flow analyses. Section 2 briefly outlines the computational procedure employed in the DLM and CPM methods. The details of the integration of the supersonic code are given

in Sections 3 and 4. Discussions of the test cases chosen to verify the integration are reported in Section 5.

2. MATHEMATICAL MODEL

This section gives a brief outline of the mathematical basis and the common features that exist between the doublet lattice and constant pressure panel methods. In these two methods, a given wing-body configuration can be represented by a number of finite elements with their side edges parallel to the freestream. The doublet lattice method (DLM) in subsonic flow and the constant pressure method (CPM) in supersonic flow assume a constant pressure within each element and determine the velocity components at user specified downwash points where the normal boundary condition is set to zero, i.e., there is no flow through the surface. The velocity at a control point j due to a unit value of pressure C_{p_i} over a panel i can be written as

$$w_{ji} = \int \int_S K_{ji} \, ds \quad (1)$$

where K_{ji} is a kernel function relating the pressure at the i th element and the normal velocity at the j th element. The analytical expression for K_{ji} in subsonic flow is given by Landahl (Reference 6) whereas the expression for supersonic flow is given by Appa (Reference 5). The details of the computation of the normal velocities are described in Reference 3 for subsonic flow and in Reference 5 for supersonic flow. A key difference in these two methods lies in the chordwise integration. The DLM code assumes an equivalent load distributed along the $1/4$ - chordline of an influencing element and computes the downwash at the $3/4$ - chord of a receiving element. In the CPM code, the chordwise integration is performed using a Gaussian quadrature integration technique with the control point chosen at 95% of the receiving

element chord. The spanwise integrations in both the methods are performed using the principal value of the singular integral. Since the pressure is zero outside of the lifting surfaces, there is no need to model the wake or the diaphragm regions, as is required in the velocity potential methods, such as Mach Box.

Once the computation is performed for all combinations of influencing and receiving elements in the zone of influence, a matrix relation between the pressure and the kinematic boundary conditions can be written as

$$[W] \{C_p\} = \frac{D\eta}{DT} \quad (2)$$

where W - influence coefficient matrix whose elements are given by Equation (1)

C_p - the pressure difference across a finite element

$\frac{D\eta}{DT} = \frac{\partial \eta}{\partial x} + i k \left(\frac{2\eta}{c} \right)$ is the kinematic boundary condition in which η

is the displacement normal to the control element and $\partial \eta / \partial x$ is the streamwise slope at that point,

$k = \frac{\omega c}{2V}$ is the reduced frequency

c - reference chord

V - aircraft velocity

Equation (2) is identical in both the subsonic (DLM) and supersonic (CPM) schemes. Hence, a common computational procedure to determine the pressures and the generalized forces has been implemented in the FASTEX code.

The influence of a body in subsonic flow is represented by source singularities along the centerline of the body together with the interference panels on the surface of the body. However, in supersonic flow the influence

of the body is represented by constant pressure panels, similar to those on the lifting surfaces, except that their strengths are halved. The body panels are assumed to have no inclination to the streamlines.

3. UPDATING OF THE FASTEX CODE

The FASTEX code is a modified version of the flutter and strength optimization computer program known as FASTOP (Reference 2). The FASTEX code retains only those features necessary for unsteady aerodynamic force computations and flutter solutions. The aerodynamic forces in subsonic flow are computed using the doublet lattice method (DLM) of Reference 3, whereas, in supersonic flow, the Mach box method of Reference 4 was originally employed.

The objective of this contract has been to provide a better supersonic airloads analysis capability in FASTEX by integrating the constant pressure panel method (CPM) of Reference 5 into it. Since the CPM approach is similar to the doublet lattice code (DLM), the updates necessary for the determination of supersonic air loads may be made using the geometrical data already prepared for a subsonic analysis.

Figure 1 shows a general layout of the FASTEX code. The RODDEN subroutine originally computed the aerodynamic influence coefficient (AIC) for subsonic flow only. Subroutines shown by hatched boundaries in Figure 1, were updated to perform the computation of the AIC matrix for supersonic flow as well. Brief descriptions of the updates made in each of the subroutines are given in the following paragraphs.

SUBROUTINE AFAM

This is a driver routine which depending on Mach number, branches either to the subsonic routine RODDEN or the supersonic routine MACH. Selection of the supersonic analysis is now deferred to subroutine PRT2. Therefore, the call to MACH in AFAM was commented out.

SUBROUTINE PART1

This routine computes the element coordinates for the DLM procedure. Necessary updates were made to compute the element corner points and the control points as required by the CPM procedure. For supersonic flow, the control point is set at 95 percent of the element average chord, whereas in subsonic flow it is at 75 percent of the element average chord. These geometric points are generated for each panel as input into FASTEX, i.e. in the XY-plane.

Two labeled common statements were added to this routine:

COMMON/XYZORD/XYZ(3,4,400)

COMMON/BODCOR/IBOD1,IBOD2

The common block XYZ contains the coordinates of the corner points of the panels as defined for use in CPM. The integers IBOD1 and IBOD2 identify the first and last of the contiguous panels which define a fuselage.

SUBROUTINE GLOBAL

Subroutine GLOBAL rotates and translates the panel corner and control points (as defined by subroutine PART1) into their final desired locations. Updates were made to the subroutine GLOBAL to perform this operation on the coordinates of the panels as defined for the CPM procedure in subroutine PART1.

SUBROUTINE PRT2

This is the driver routine to compute the AIC matrix. Necessary updates were made to generate the local coordinates of a sending element with respect to a control point. For supersonic flow, a calling statement was introduced to access the CPM subroutine.

The COMMON cards added are:

COMMON/XYZORD/XYZ(3,4,400)

COMMON/BODCOR/IBOD1,IBOD2

SUBROUTINE CPM

This is the driver routine used for the computation of the supersonic downwash factor W_{ji} , at a control point j due to a unit pressure on sending element i . A coordinate transformation is performed using the XYZM subroutine to rotate the sending element such that it is parallel to the XY-plane. The supersonic kernel functions are evaluated first by applying numerical integration in the chordwise direction and then by an analytical integration in the spanwise direction. The computation of W_{ji} takes into consideration the symmetry condition about the $y = 0$ plane. However, no ground effect option is included in the coding.

The computation of the downwash factors W_{ji} due to the lifting pressures on body panels is also performed for all elements numbered from IBOD1 through IBOD2. Centerline fins are assumed to carry half of the computed total load for the antisymmetric boundary condition, while they carry the total load for the asymmetric boundary conditions.

Input Parameters:

IE Receiving element

XYZC Coordinates of the downwash control point in the receiving
 element

JE Influencing element

XYZS Corner coordinates of the influencing element

ISYMS Flag for structural symmetry about the $y = 0$ plane
 0 - no symmetry
 1 - symmetry

ISYMA Flag for aerodynamic symmetry about $y = 0$ plane
 0 - no symmetry
 1 - symmetry
 -1 - antisymmetry

DC Direction cosines of the normals of the influencing and
 receiving panels

M Mach No.

BT $\beta = \sqrt{M^2 - 1}$

PI π

XKO k (reduced frequency) = $\frac{\omega \text{ REFL}}{V}$

REFL Reference length

Output Parameter:

WIJ Downwash factor at element IE due to a unit pressure over
 element JE

SUBROUTINE XYZM

This routine transforms the sending element coordinates such that the influencing element is parallel to the XY-plane. The reference origin is at the downwash point of a receiving element. This routine also determines whether the influencing element is within the forward Mach cone or outside the zone of influence. This routine is called from the CPM module.

SUBROUTINE FUNC2

This routine performs the spanwise integration of a dipole singular function of the type $F(\eta)/(\eta^2 + \zeta^2)$ and is called from the CPM module.

SUBROUTINE FUNC4

This routine performs spanwise integration of a quadrupole singular function of the type $F(\eta)/(\eta^2 + \zeta^2)^2$ and is called from the CPM module.

4. INPUT DATA MODIFICATIONS

The similarity of the CPM and DLM codes allows for a common set of input data. The only change required in the DLM input is for the identification of body panels. The identification of body panels is specified by the NB parameter in the following input entry (card image).

DATA:	NDELT	NP	NB	NCORE	N3	N4	N7
FORMAT:	(I5)	(I5)	(I5)	(I5)	(I5)	(I5)	(I5)

NB - 0 denotes that there are no body panels

NB - 1 denotes that there are body panels for a subsonic case. Input is as per that required for a DLM analysis.

NB - -1 denotes that there are body panels for a supersonic case. The above input is then immediately followed by an input specifying the beginning and ending panel identifiers of the contiguous panels which describe the body:

DATA:	IBOD1	IBOD2
FORMAT:	(I5)	(I5)

IBOD1 is the beginning panel identifier of the body

IBOD2 is the ending panel identifier of the body

If NB - 0 or 1, the IBOD1, IBOD2 entry is omitted. If NB - -1, input for bodies subsequent to the IBOD1, IBOD2 entry, is omitted, except for that which define body panel coordinates and modal grid points. A typical example of the input data of an aircraft configuration with a body in supersonic flow is given in Figure 2.

5. VERIFICATION OF THE SUPERSONIC CODE IN FASTEX

To verify proper integration of the supersonic CPM with the subsonic DLM analysis procedure, the following test cases were exercised:

- (1) A Cornell Flutter Model (Reference 9)
- (2) The X-29 forward swept wing aircraft
- (3) An oblique wing research aircraft

The following is the discussion of the results of these test cases.

5.1. The Cornell Flutter Model

The Cornell flutter model shown in Figure 3 was chosen to verify the predicted pressure distributions and flutter characteristics by comparison with the available analytical and experimental data. The planform was represented by 20 spanwise panels and 10 chordwise panels. Computations were performed at two Mach numbers, viz., $M = 1.135$ and $M = 1.2$. The pressure distributions at 75 percent of the wing span for these two Mach numbers, together with data from another source (Reference 7) are shown in Figures 4 and 5.

The solid line in these figures denotes the pressure distribution predicted by the Mach box method (Reference 4), while the data denoted by the circular and square symbols were obtained from the linearized and nonlinear versions of XTRAN3S (Reference 8), respectively. Near the leading edge, the CPM predicted data correlates well with the linear model of XTRAN3S, while near the trailing edge the CPM shows an average of the linear and the nonlinear data. The unsmoothed Mach box data shows an oscillatory variation which has an average distribution well above other results.

The wind tunnel model described in Reference 9 was used to verify the accuracy of flutter speed predictions. The CPM predicted flutter speed and the corresponding frequencies, using three vibration modes and various numbers of boxes, are shown in Figure 6. The convergence is seen to be very rapid. The predicted flutter speeds with a 10 x 20 box arrangement are compared with the experimental data of Reference 9 in Table A. For a density ratio $\rho/\rho_0 = 0.2481$, the predicted flutter speed is 0.42 percent conservative, and for the density ratio $\rho/\rho_0 = 0.2607$, it is 2.65 percent unconservative.

5.2 Stability Derivatives of the X-29 Aircraft

To evaluate the accuracy of the supersonic module (CPM), the X-29 was modeled as shown in Figure 7 with 90 body panels and 211 lifting panels. The longitudinal and lateral stability derivatives were computed at Mach numbers $M = 1.05$ and 1.2 . The results were compared with the NASA supplied data of Reference 10.

Table 3 shows the comparison of longitudinal stability derivatives of a rigid X-29 aircraft with those of Reference 10. The lift curve slope C_{L_α} compares very well, while the pitching moment coefficient C_M shows some difference. However, since the aerodynamic center is very close to the reference pitch axis, a small variation in the aerodynamic center would account for a large variation in the pitching moment. Thus, a more meaningful item of comparison would be the location of the aerodynamic center itself. The variation in the location of the aerodynamic center between the present prediction and the reference data is less than 2 inches, which is about 2.3% of the mean aerodynamic chord. The lift and moment derivatives due to canard, strake and flap are all seen to be in reasonable agreement with those of Reference 10, except for the canard lift coefficient at $M = 1.05$, which is

approximately half that of Reference 10. This variation may arise from the Mach wave interference with the fuselage intake, which has not been modeled.

The dynamic derivatives $C_{M_{\dot{\alpha}}}$, C_{L_q} and C_{M_q} also agree reasonably well with the referenced data, while the $C_{L_{\dot{\alpha}}}$ term is significantly different both in sign and magnitude. In order to examine this discrepancy, a parabolic displacement mode was used to calculate the C_{L_q} and C_{M_q} terms.

The computation of C_{L_q} from unsteady data is determined from the following expression:

$$C_{L_q} = \frac{2(Q_{12})_I}{kS} - C_{L_{\dot{\alpha}}}$$

The alternative approach, using a steady camber mode deformation on the whole airplane, is given by the following expression:

$$C_{L_q} = \frac{2(Q_{13})_R}{S}$$

where

$(Q_{12})_I$ - Imag (Lift due to pitch)

$(Q_{13})_R$ - Real (Lift due to camber)

The C_{L_q} and C_{M_q} values determined in this manner agreed exactly with the results obtained from the unsteady data (which are dependent on $C_{L_{\dot{\alpha}}}$). Hence the $C_{L_{\dot{\alpha}}}$ predicted by CPM is considered to be reasonable and suggest an error in the Reference 10 value.

Table 4 shows the comparison of the lateral stability derivatives. Once again, the rate and control derivatives are seen to be in reasonable agreement with the referenced data except for the following four derivatives: $C_{n_{\dot{\beta}}}$, $C_{n_{\dot{\beta}}}$, C_{n_r} and C_{n_p} .

In conclusion, the predicted X-29 stability derivatives are seen to be in reasonable agreement with Reference 10.

5.3. Stability Derivatives of an Oblique Wing Research Aircraft

To verify the asymmetric capability of the CPM/FASTEX code, an analysis was performed on the 200 ft² (wing area) oblique wing research aircraft to determine the stability derivatives of the aircraft. The complete aircraft was represented by 308 elements, with 180 elements on the body, 68 elements on the wing, 30 elements on the horizontal tail and 30 elements on the vertical fin. This is a somewhat simplified model due to limitations on the number of elements in the FASTEX code. For improved accuracy it is recommended that the total aircraft be represented by a minimum of 600 elements. Figure 7 shows the computer model used in the analysis. To determine the stability derivatives, eight displacement modes were used representing 5 rigid body modes and 3 control surface deflections. The wing was set at a sweep angle of 55 degrees and a dihedral angle of 5 degrees. No streamwise inclination of the wing was considered because the FASTEX code employs the linearized boundary conditions, which uncouple the incidence and sideslip angles, as discussed below.

The nonlinear boundary condition can be written as,

$$\frac{DN}{DT} = (\cos\alpha \cos\beta n_x - \sin\beta n_y + \sin\alpha \cos\beta n_z) + i k \eta$$

where α - angle of attack

β - sideslip angle

n_x, n_y, n_z are the direction cosines of the normal of an element at the control point

η - deflection normal to an element

k - reduced frequency

The linearized boundary condition for small values of α and β , is

$$\frac{DN}{DT} = (n_x - \beta n_y + \alpha n_z) + i k \eta$$

This eliminates the coupling between the sideslip angle β and the angle of incidence n_x . Hence the cross derivatives, such as lift and pitching moment due to β , will not be predicted accurately if the wing is geometrically inclined to the freestream.

Table 4 compares the stability derivatives computed for this configuration using the CPM code with the data reported in Reference 10. The rotary derivatives were reportedly obtained by theoretical means while the static derivatives were obtained from wind tunnel tests. Although a simplified model was used, the derivatives, except for rudder effectiveness, are shown to agree reasonably well with those of Reference 11. The cross derivatives side force due to pitch rate, pitching moment due to sideslip, and rolling moment due to pitch rate, etc., show significant differences. The discrepancy associated with the rudder effectiveness may arise due to; (a) poor modeling because of limitations on the number of panels, (b) viscous effects which modify the flow characteristics along the trailing edges when deflected, and (c) a possible error reported in Reference 11.

6. CONCLUSIONS AND RECOMMENDATIONS

The CPM module has been integrated into the NASA/Ames version of the FASTEX code. The resulting unified code permits the determination of unsteady airloads both in subsonic and supersonic flow regimes.

The accuracy of the integrated code was demonstrated by comparing the pressure distributions, stability coefficients and flutter solutions, with the available data.

Experience in the use of the FASTEX code has revealed the following limitations:

1. The size of the problem can be modeled with the FASTEX code is limited to 320 panels, although users manual claims to accommodate 400 panels. This limitation needs to be revised for modeling an aircraft with a large number of panels.
2. The flutter module fails to predict close roots. Hence this module should be updated.
3. The interpolation routine does not predict accurate slopes for higher order vibration modes.
4. The restart option does not function properly. This is a very cost effective option for aeroelastic analyses using different modal data and hence needs to be corrected.

The correlations shown here, as well as others obtained by the authors, suggest that the CPM code is an improvement over the traditional Mach Box method for the prediction of unsteady supersonic airloads. It is hoped that

this integration with the FASTEX System will encourage the use of this capability in further correlation studies of the CPM code on other configurations.

TABLE 1. CORNELL WING FLUTTER ANALYSIS AND TEST CORRELATION

Model	Mach	ρ/ρ_o	$V_{f\text{exp}}$	$V_{f\text{calc}}$ (CPM)	$\omega_{f\text{exp}}$	$\omega_{f\text{calc}}$ (CPM)
4	1.098	0.2481	708	705	69	70
5	1.135	0.2607	717	736	63	68

TABLE 2. X-29 LONGITUDINAL STABILITY DERIVATIVES (RIGID A/C)

	M = 1.05		M = 1.2	
	REFERENCE 1	PRESENT (CPM)	REFERENCE 1	PRESENT (CPM)
A/C PITCH*:				
$C_{L\alpha}$	0.1073	0.0982	0.0971	0.097
$C_{M\alpha}$	0.0156	0.0125	0.0087	0.0068
CANARD:				
$C_{L\delta c}$	0.0118	0.0067	0.0099	0.0102
$C_{M\delta c}$	0.0158	0.0155	0.0143	0.0139
STRAKE:				
$C_{L\delta s}$	0.0029	0.0032	0.0039	0.0027
$C_{M\delta s}$	-0.0051	-0.0075	-0.0062	-0.0063
FLAP:				
$C_{L\delta f}$	0.0154	0.0197	0.015	0.0162
$C_{M\delta f}$	-0.0121	-0.0135	-0.0139	-0.0132
$C_{L\dot{\alpha}}$	0.4165	-11.138	0.3854	-7.896
$C_{M\dot{\alpha}}$	-1.504	-2.94	-1.527	-1.57
C_{Lq}	7.49	6.483	6.145	4.736
C_{Mq}	-9.568	-9.123	-8.727	-8.863
* CENTER OF PRESSURE (Relative to Pitch Axis):				
X_{cp} (in)	12.6	11.03	7.765	6.075

Ref. Area = 26640 in², Ref. Chord = 86.67 in, Ref. Span = 326.4 in

A/C Pitch Axis: $X_0 = 448.77$ in, $Z_0 = 61.0$ in

Canard Pitch Axis: $X_0 = 372.2$ in, $Z_0 = 61.0$ in

Dynamic derivatives are per radian, while all others are per degree.

TABLE 3. X-29 LATERAL STABILITY DERIVATIVES (RIGID A/C).

	M = 1.05		M = 1.2	
	REFERENCE 1	PRESENT (CPM)	REFERENCE 1	PRESENT (CPM)
$C_{Y\beta}$	-0.0202	-0.0205	-0.0215	-0.0196
$C_{L\beta}$	-0.0016	-0.0028	-0.0019	-0.0026
$C_{n\beta}$	0.0044	0.0089	0.0049	0.0086
$C_{Y\dot{\beta}}$	-	-0.0023	-	0.0273
$C_{L\dot{\beta}}$	-	0.0739	-	0.0469
$C_{n\dot{\beta}}$	0.0054	-0.2197	0.006	-0.2279
C_{Yr}	-	1.5402	-	1.4534
C_{Lr}	0.237	0.2559	0.2207	0.2386
C_{nr}	-0.2563	-0.9648	-0.469	-0.8851
C_{Lp}	-0.4723	-0.4351	-0.515	-0.4659
C_{np}	0.0484	0.0659	0.0658	0.0218
$C_{Y\delta a}$	-0.0062	-0.0039	-0.0059	-0.0036
$C_{L\delta a}$	0.002	0.0016	0.0013	0.0014
$C_{n\delta a}$	0.0012	0.002	0.0017	0.0019
$C_{Y\delta r}$	0.0028	0.0031	0.0016	0.0019
$C_{L\delta r}$	0.00056	0.00071	0.0003	0.00045
$C_{n\delta r}$	-0.0017	-0.0021	-0.0011	-0.0013

Ref. Area = 26640 in², Ref. Chord = 86.67 in, Ref. Span = 326.4 in
A/C Yaw Axis: $X_0 = 448.77$ in, $Y_0 = 0.0$ in
Dynamic derivatives are per radian, while all others are per degree.

TABLE 4. STABILITY DERIVATIVES OF OBLIQUE WING RESEARCH AIRCRAFT (RIGID A/C)

Mach No. = 1.2

	Rolling Moment	Pitching Moment	Yawing Moment	Lift	Side Force	Source
Roll rate (pb/2V) (rad/sec)	-0.154 -0.155	1.988 1.616	0.0928 0.1374	0.1748 -0.0067	-0.39 -0.328	Ref. 1 CPM
Pitch rate (qc/2V) (rad/sec)	1.257 -0.0436	-98.07 -107.84	0.539 0.3264	16.702 21.22	0.18 -0.9914	Ref. 1 CPM
Yaw rate (rb/2V) (rad/sec)	0.1627 0.1808	-0.0223 0.1853	-0.875 -0.678	0.115 0.085	2.02 2.174	Ref. 1 CPM
alpha α (rad)	0.0985 0.1098	-4.749 -3.768	-0.0908 -0.0395	4.943 4.204	-0.365 0.2208	Ref. 1 CPM
beta β (rad)	-0.123 -0.211	1.191 0.7339	0.3396 0.4544	-0.446 -0.2299	-2.139 -1.927	Ref. 1 CPM
left horizontl δ_{lh} (rad)	0.0397 0.0596	-2.06 -2.569	0.0379 0.00003	0.4536 0.6006	-0.0882 0.00007	Ref. 1 CPM
right horizntl δ_{rh} (rad)	-0.0392 -0.0597	-2.06 -2.569	-0.0378 -0.00003	0.4536 0.6006	0.0882 -0.00007	Ref. 1 CPM
Rudder δ_r (rad)	0.0165 0.066	0.033 0.0029	-0.068 -0.2261	0 -0.0004	0.1501 0.4744	Ref. 1 CPM

Ref. Area = 200 ft², Ref. Chord = 4.778 ft, Ref. Span = 45.12 ft

A/C Pitch Axis: $X_0 = 454.0$ in $Z_0 = 100.0$ in

A/C Yaw Axis: $X_0 = 454.0$ in $Y_0 = 0.0$ in

Horizontal Tail Pitch Axis: $X_0 = 663.501$ in $Z_0 = 92.0$ in

$C_{N\dot{\alpha}} = 0.2254$ (CPM), $C_{m\dot{\alpha}} = -1.037$ (CPM)

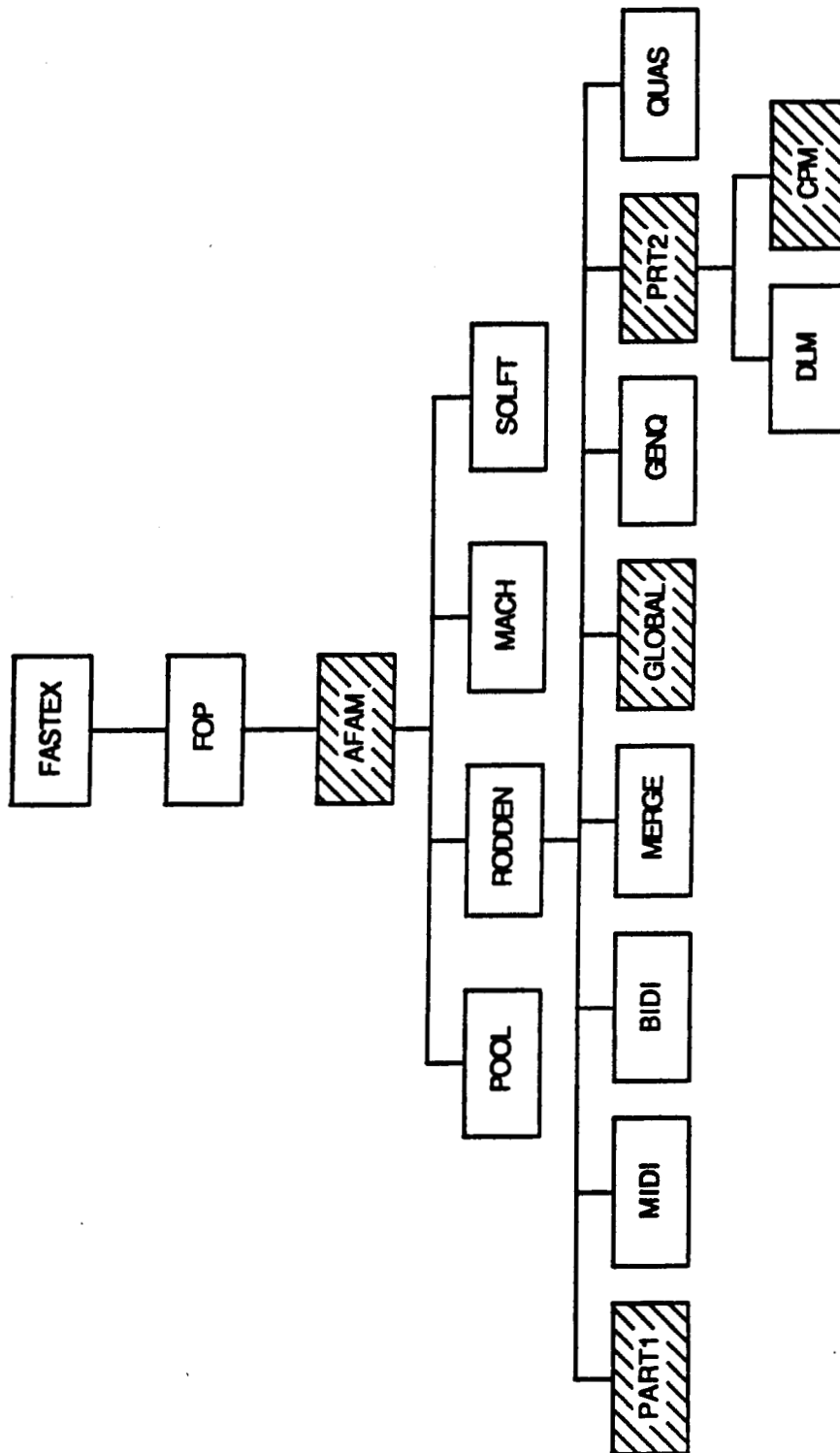


Figure 1. Schematic Diagram of Enhanced FASTEX Code

ALTITUDE: SEA LEVEL

MODIFICATIONS FOR BODY PANELS IN SUPERSONIC FLOW

24

			90.0		
580.565	672.000	665.464	690.625	96.0	177.00
0.0	0.0	8 6	0.0		
0.0	0.2	0.41695	0.63390	0.81695	1.0
0.0	0.17161	0.28571	0.42857	0.57143	0.71428
0.87654	1.0				
333.37	439.665	333.37	448.759	20.00	37.50
61.0	61.0	3 7	0.0		
0.0	0.16667	0.33333	0.5	0.66667	0.83333
1.0					
0.0	0.50	1.00			
333.37	424.66	373.230	402.260	37.50	81.771
61.0	61.0	6 6	0.0		
0.0	0.20	0.40	0.60	0.80	1.00
0.0	0.20	0.40	0.60	0.80	1.00
439.665	669.220	452.656	669.220	20.0	45.0
61.0	61.0	4 14	0.0		
0.0	0.07692	0.15385	0.23077	0.30769	0.38462
0.46154	0.53846	0.61538	0.69231	0.76923	0.86931
0.92307	1.00				
0.0	0.35	0.7	1.00		
452.656	571.745	463.626	552.931	45.0	64.0
61.0	61.0	3 9	0.0		
0.0	0.125	0.25	0.375	0.5	0.625
0.7725	0.875	1.0			
0.0	0.5	1.0			
463.626	552.931	408.010	455.991	64.0	163.22
61.0	61.0	13 8	0.0		
0.0	0.14286	0.28571	0.42857	0.57143	0.75
0.85714	1.0				
0.0	0.08333	0.16667	0.25	0.33333	0.41667
0.5	0.58333	0.66667	0.75	0.83333	0.93953
1.0					
0.0	0.0	96.0	-36.87		
153.00	669.22	153.000	669.22	0.0	25.0
0.0	0.0	2 31	0.0		
0.0	0.03333	0.06667	0.1	.133333	.166667
0.2	0.23333	0.26667	0.3	.333333	.349405
0.38476	0.42014	0.4555	0.49088	.526248	.555315
0.59186	0.62842	0.66497	0.70152	.73807	.77462
.8112	0.84265	0.87412	0.90558	.93706	.96853
1.0					
0.0	1.0				
0.0	20.0	81.0	-90.0		
153.00	669.22	153.000	669.22	0.0	20.0
0.0	0.0	2 31	0.0		
0.0	0.03333	0.06667	0.1	.133333	.166667
0.2	0.23333	0.26667	0.3	.333333	.349405
0.38476	0.42014	0.4555	0.49088	.526248	.555315
0.59186	0.62842	0.66497	0.70152	.73807	.77462
.8112	0.84265	0.87412	0.90558	.93706	.96853
1.0					
0.0	1.0				

BODY PANELS

Figure 2. FASTEX Input Data Format Using Body Panels in Supersonic Flow. (Continued).

0.0	20.0	61.0	-153.435		
153.00	669.22	153.000	669.22	0.0	22.3607
0.0	0.0	2 31	0.0		
0.0	0.03333	0.06667	0.1	.133333	.166667
0.2	0.23333	0.26667	0.3	.333333	.349405
0.38476	0.42014	0.4555	0.49088	.526248	.555315
0.59186	0.62842	0.66497	0.70152	.73807	.77462
.8112	0.84265	0.87412	0.90558	.93706	.96853
1.0					
0.0	1.0				
1	0	0	7	35	0
F	35	0			
2	0	0	0		
2	580.565	96.0	665.464	177.0	
	96.0	177.0			
2	672.0	96.0	690.625	177.0	
	96.0	177.0			
F	12	0			
2	0	0	0		
2	333.37	20.0	333.37	37.5	
	20.0	37.5			
2	439.665	20.0	448.759	37.5	
	20.0	37.5			
F	25	0			
2	0	0	0		
2	333.37	37.5	373.23	81.771	
	37.5	81.771			
2	424.66	37.5	402.26	81.771	
	37.5	81.771			
T	39	1			
2	0	0	0		
2	439.665	20.0	452.656	45.0	
	20.0	45.0			
2	669.22	20.0	669.22	45.0	
	20.0	45.0			
639.22	20.0	640.92	45.0		
2	0	0	0		
2	639.22	20.0	640.92	45.0	
	20.0	45.0			
2	669.22	20.0	669.22	45.0	
	20.0	45.0			
T	16	1			
2	0	0	0		
2	452.656	45.0	463.626	64.0	
	45.0	64.0			
2	571.745	45.0	552.931	64.0	
	45.0	64.0			
544.652	45.0	532.614	64.0		
2	0	0	0		
2	544.652	45.0	532.614	64.0	
	45.0	64.0			
2	571.745	45.0	552.931	64.0	
	45.0	64.0			

Figure 2. FASTEX Input Data Format Using Body Panels in Supersonic Flow (Continued).

```

T  84  1
2  0  0  0
2  463.626  64.0  408.010  163.22
   64.0  163.22
2  552.931  64.0  455.991  163.22
   64.0  163.22
530.605  64.0  449.000  157.22
2  0  0  0
2  530.605  64.0  449.000  157.22
   64.0  157.22
2  552.931  64.0  460.952  157.22
   64.0  157.22
F  30  0
2  0  0  0
2  153.000  0.0  153.000  20.0
   0.0  20.0
2  669.220  0.0  669.220  20.0
   0.0  20.0
F  30  0
2  0  0  0
2  153.000  0.0  153.000  20.0
   0.0  20.0
2  669.220  0.0  669.220  20.0
   0.0  20.0
F  30  0
2  0  0  0
2  153.000  0.0  153.000  20.0
   0.0  20.0
2  669.220  0.0  669.220  20.0
   0.0  20.0
1

```

Figure 2. FASTEX Input Data Format Using Body Panels in Supersonic Flow (Concluded).

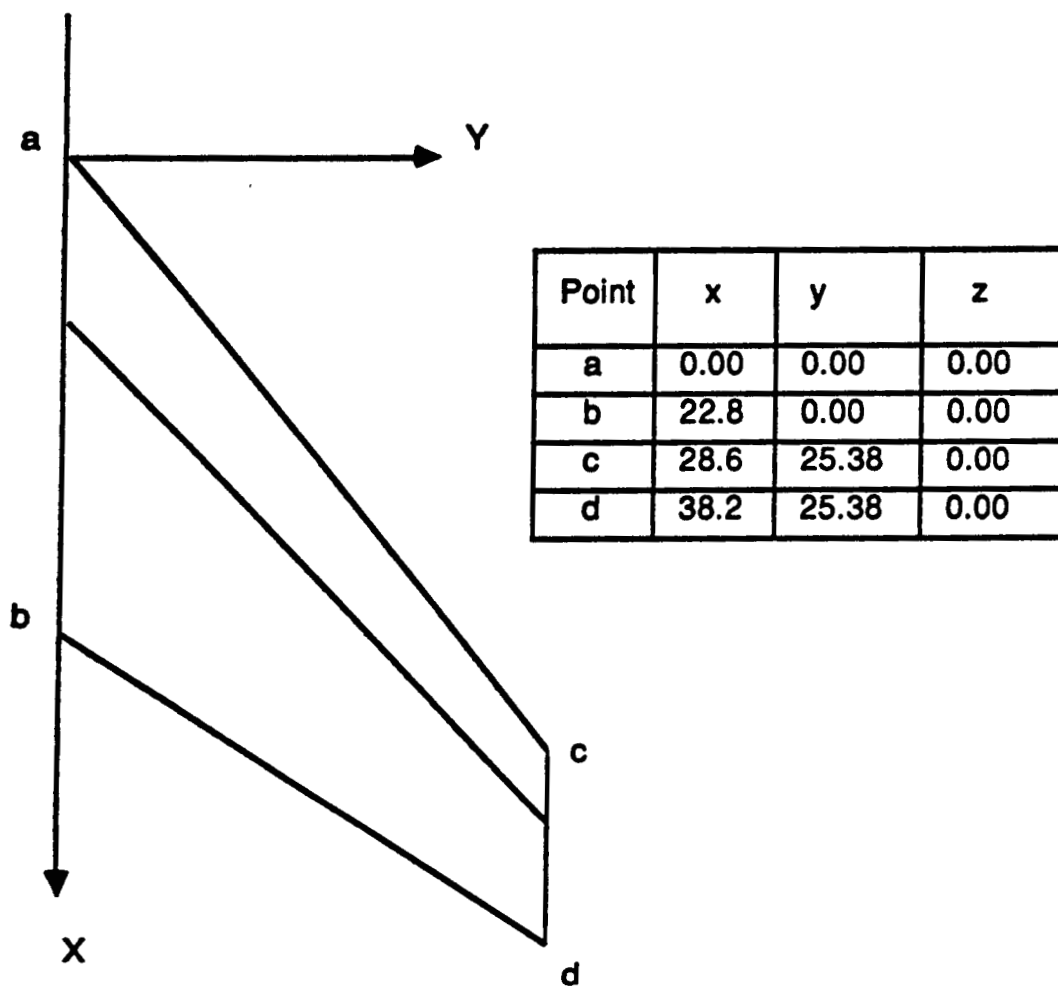


Figure 3. Planform of the Cornell Flutter Model

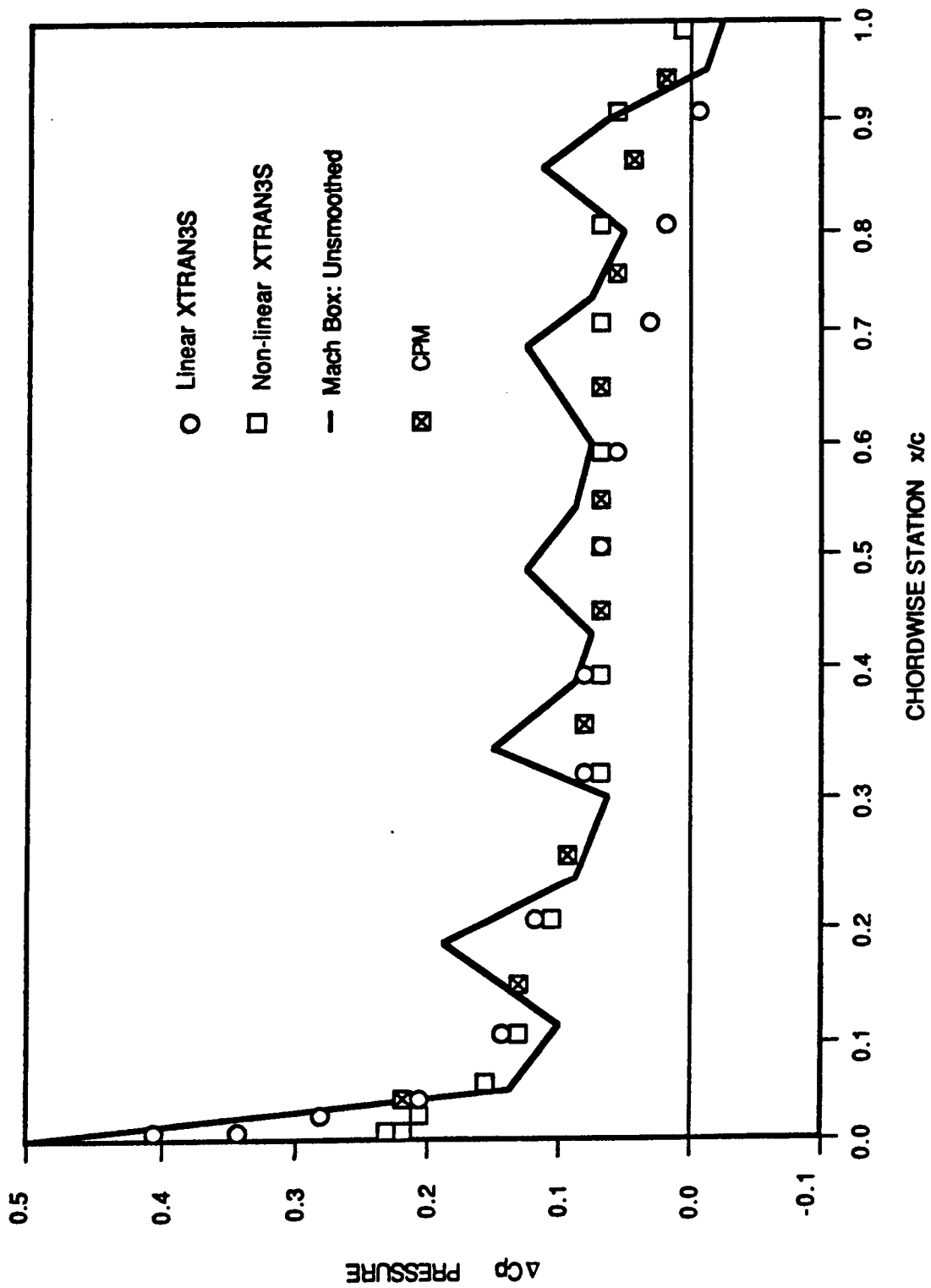


Figure 4. Chordwise Pressure Distribution on the Cornell Wing

$M = 1.135$ $y/b = 0.75$

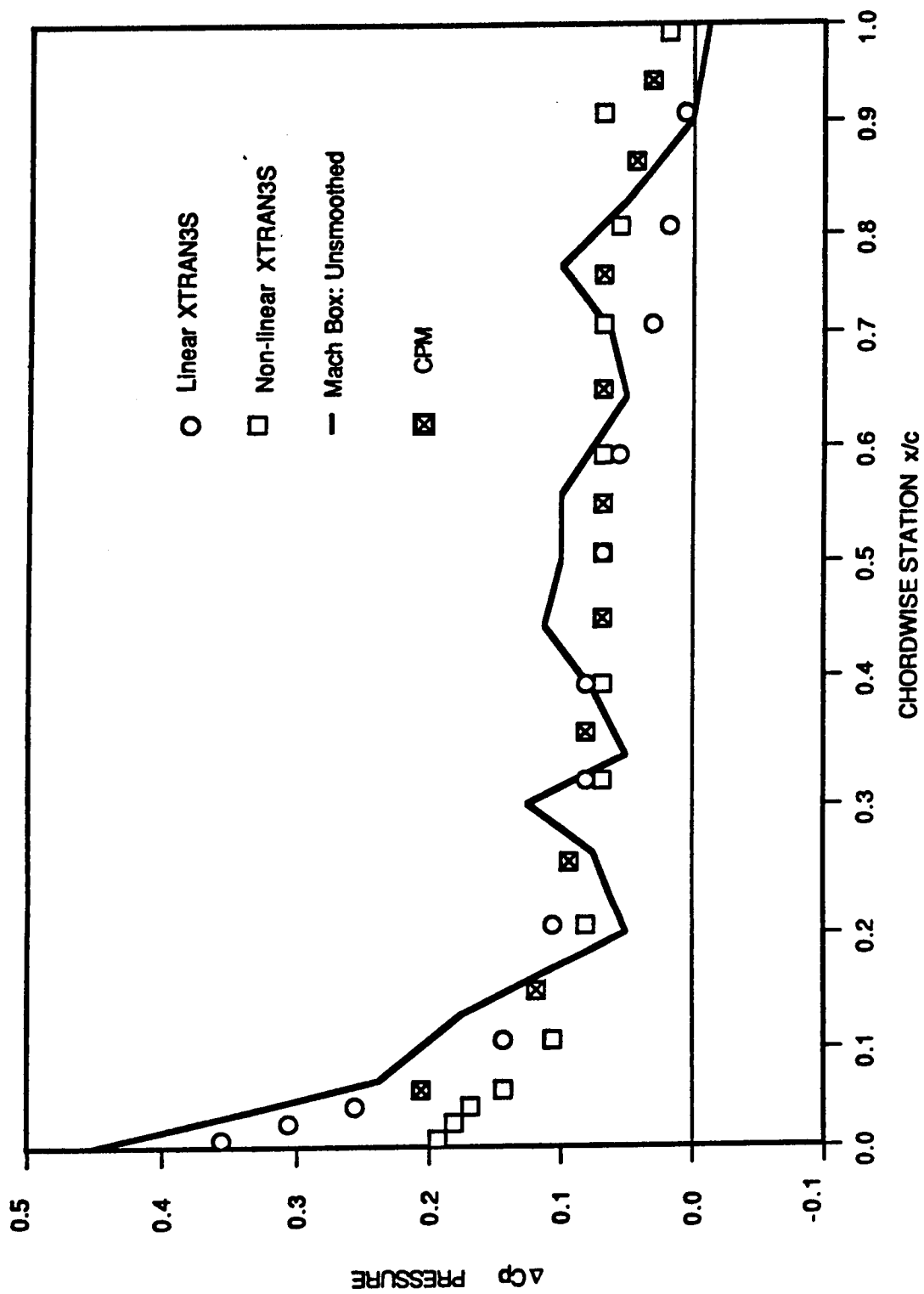


Figure 5. Chordwise Pressure Distribution on the Cornell Wing

$M = 1.2$ $y/b = 0.75$

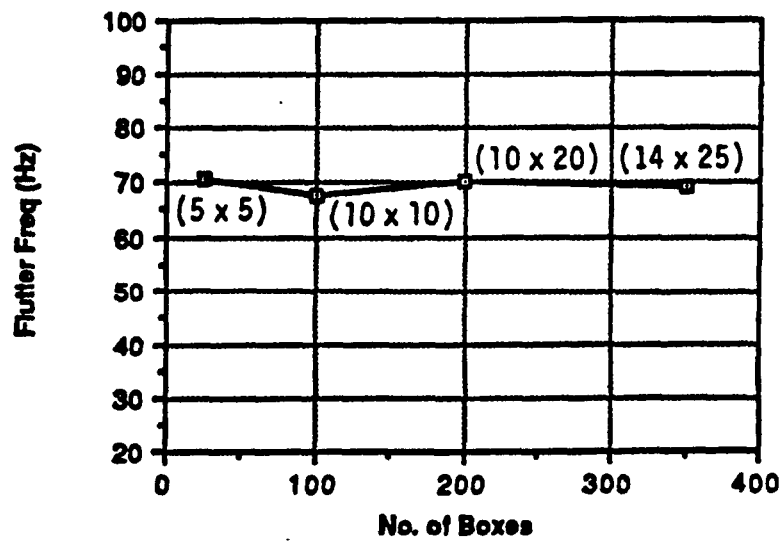
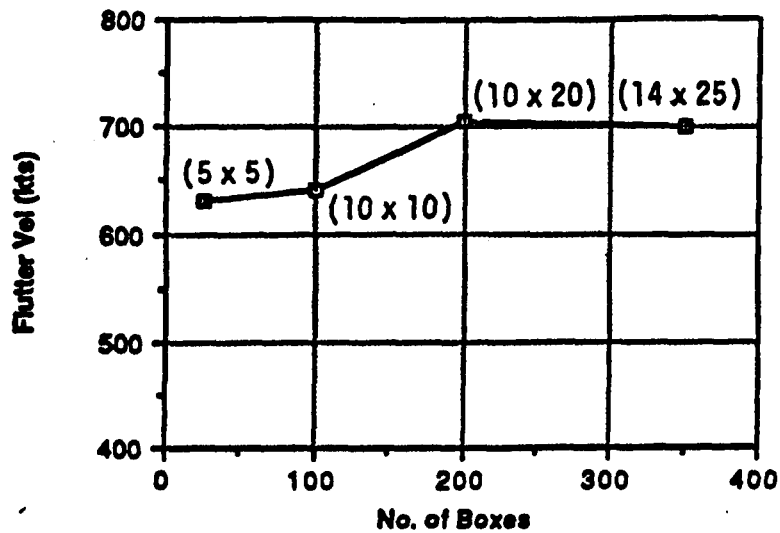


Figure 6. Flutter Speed and Frequency Versus Number of Boxes Used in the CPM Code.

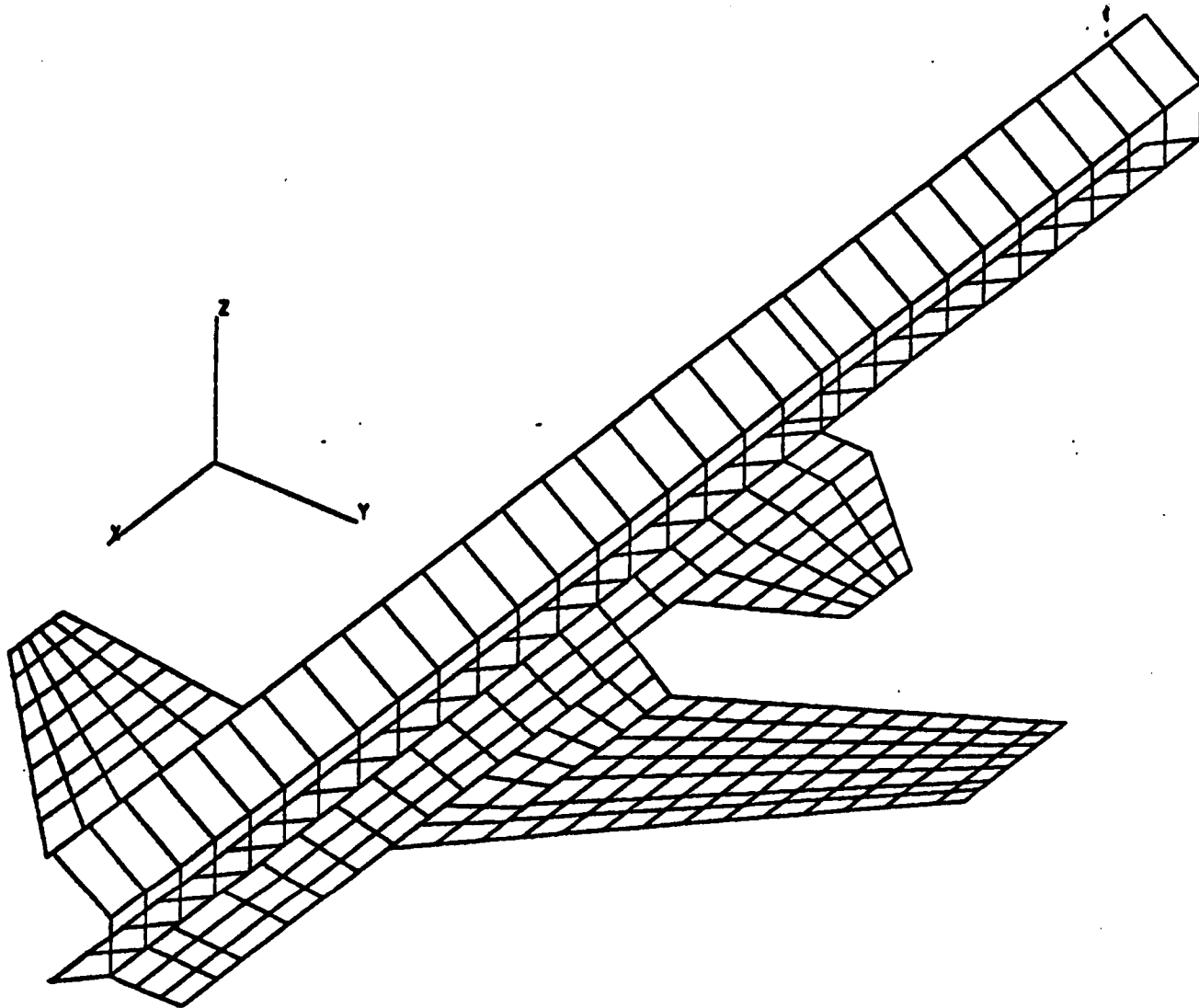


Figure 7. X-29 Modelling for Unsteady Airloads Predictions.

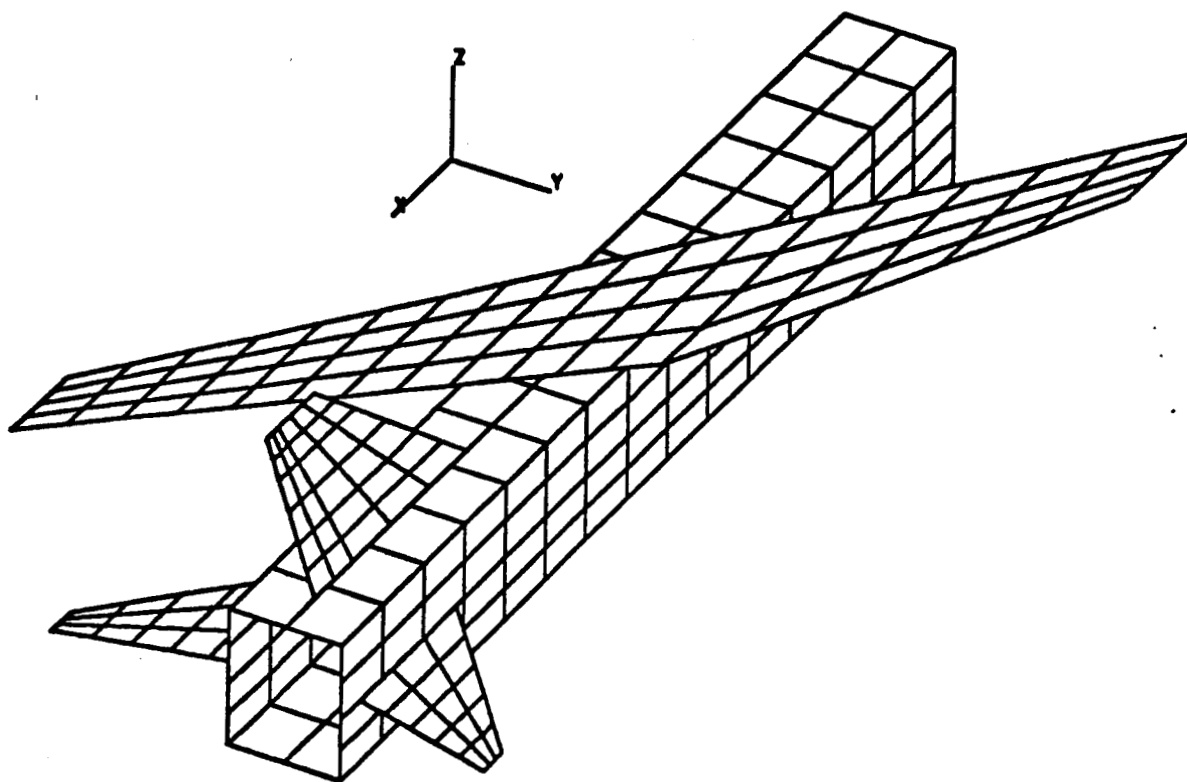


Figure 8. Computational Model of an Oblique Wing Research Aircraft.

REFERENCES

1. Taylor, R. F., Miller, K. L. and Brockman, R. A., "A Procedure for Flutter Analysis of FASTOP-3 Compatible Mathematical Models," Volume 1 - Theory and Application, AFWAL-TR-81-3063, June 1981.
2. Markowitz, J., and Isakson, G., "FASTOP-3: A Strength, Deflection and Flutter Optimization Program for Metallic and Composite Structures," Vol. I - Theory and Application, Vol. II - Program User's Manual, AFFDL-TR-78-50, May 1978.
3. Giesing, J. P., Kalman, T. P., and Rodden, W. P., "Subsonic Unsteady Aerodynamics for General Configurations. Part I, Vol. I, Direct Application of the Nonplanar Doublet-Lattice Method" Vol. II, Computer Program H7WC, Air Force Flight Dynamics Laboratory Technical Report, AFFDL-TR-71-5, Part I, November 1971.
4. Li, J. M., Borland, C. J., and Hogley, J. R., "Prediction of Unsteady Aerodynamic Loadings of Nonplanar Wings and Wing-Tail Configurations in Supersonic Flow; Part 1, Theoretical Development, Program Usage and Application," AFDDL-TR-71-108, Part I, March 1972.
5. Appa, K., "Constant Pressure Panel Method for Supersonic Unsteady Airloads Analysis," Journal of Aircraft, Vol. 24, No. 10, 1987, pp. 696-702.
6. Landahl, M.T., "Kernel Function for Nonplanar Oscillating Surfaces in a Subsonic Flow," AIAA Journal, Vol. 5, May 1967, pp. 1045-1046.
7. Huttshell, L. Private Communication, Sept. 1987.
8. Borland, C. J., "XTRAN3S - Transonic Steady and Unsteady Aerodynamics for Aeroelastic Applications, Volume I - Technical Development Summary," AFWAL-TR-85-3124, Vol. I, January 1986.

9. Maier, H., and King, S., "Transonic Flutter Model Tests," Part One, 45° Swept Wings, WADC Technical Report 56-214, Wright Air Development Center, Wright-Patterson Air Force Base, Ohio, September 1957.
10. Frei, D. and Moore, M., "X-29 High Angle of Attack, Flexible, Nonlinear Aerodynamic Math Model (Aero 7); Data Tables," Grumman Aircraft Corporation Memo No. 712/ENG-M-84-161, May 8, 1984.
11. Yamamoto, T. G., Wong, H. W. and Chung, D. K., "F-8 Oblique Wing Feasibility Study Extension-Final Report," NA-84-2097, November 1984.
12. Roukis, D., "X-29 Supersonic Flutter Analysis Based on Ground Vibration Survey Data," GAC 712-ENG-RPT-85-004, Dec. 5, 1985. Grumman Aerospace Corporation, Bethpage, New York.